Journal of Food Measurement and Characterization (2021) 15:4617–4622
https://doi.org/10.1007/s11694-021-01027-0

ORIGINAL PAPER

High performance of screen-printed graphite electrode modified with Ni–Mo-MOF for voltammetric determination of amaranth

Somayeh Tajik[1] · Yasin Orooji[2,3] · Fatemeh Karimi[4] · Zohreh Ghazanfari[5] · Hadi Beitollahi[6] · Mohammadreza Shokouhimehr[7] · Rajender S. Varma[8] · Ho Won Jang[7]

Received: 15 February 2021 / Accepted: 15 June 2021 / Published online: 28 June 2021

Abstract

The present study introduces a novel Ni–Mo-MOF-modified screen printed electrode (Ni–Mo-MOF/SPE) to sensitively and rapidly detect amaranth. Cyclic voltammetry (CV) was also applied to evaluate the electrochemical behavior of amaranth on the surfaces of bare SPE and Ni–Mo-MOF/SPE, and differential pulse voltammetry (DPV) to calculate linearly detection range of amaranth. According to the results, various linear oxidation peak currents were obtained at different concentrations (between 0.15 ± 0.001 and 500.0 ± 0.001 µM) and the limit of detection (LOD) was estimated to be 0.05 ± 0.001 µM in the optimal conditions. Additionally, the efficacy of developed electrode was tested by real samples, the results of which were satisfactory. The proposed Ni–Mo-MOF/SPE not only had special properties such as high selectivity, high sensitivity, cost-effectiveness and rapid response, but also was shown to possess wide applications for sensitively amaranth detection in real samples.

Keywords Screen printed graphite · Modified electrode · Voltammetric detection · Amaranth

Introduction

Aromatic azo dyes are by far the most substantial class of organic colorants widely exploited in different industries such as cosmetics, drug, agricultural and food fields. Such industries discharge wastewater containing large quantities of dyestuffs with chemically complex features and high concentrations [1, 2]. 3-hydroxy-4-[(4-sulfo-1-naphthalenyl)azo]-2,7-naphthalenedisulfonic acid trisodium salt, amaranth, is a synthetic water-soluble red pyrazolone dye and suitable for the improvement of attraction and appearance in some foods and soft drink. Nevertheless, additional consumption of amaranth can reportedly result in some health side effects, including impaired pediatric mental development, restlessness of children and childhood hyperactivity disorder [3, 4]. Patients taking aspirin and benzoic acid may be harmed by using this dye. The amaranth can also be associated with asthma and hypersensitivity [5–7].

✉ Somayeh Tajik
tajik-s1365@yahoo.com

✉ Yasin Orooji
yasin@njfu.edu.cn

✉ Hadi Beitollahi
h.beitollahi@yahoo.com

[1] Research Center for Tropical and Infectious Diseases, Kerman University of Medical Sciences, Kerman, Iran

[2] College of Materials Science and Engineering, Nanjing Forestry University, 159 Longpan Road, Nanjing 210037, People's Republic of China

[3] Co-Innovation Center of Efficient Processing and Utilization of Forest Resources, Nanjing Forestry University, Nanjing 210037, China

[4] Department of Chemical Engineering, Quchan University of Technology, Quchan, Iran

[5] Department of Food Science, Islamic Azad University, Bam Branch, Bam, Iran

[6] Environment Department, Institute of Science and High Technology and Environmental Sciences, Graduate University of Advanced Technology, Kerman, Iran

[7] Department of Materials Science and Engineering, Research Institute of Advanced Materials, Seoul National University, Seoul 08826, Republic of Korea

[8] Regional Centre of Advanced Technologies and Materials, Palacký University in Olomouc, Šlechtitelů 27, 783 71 Olomouc, Czech Republic

Accordingly, the amaranth needs to be sensitively and easily determined by effective methods. There are currently some techniques for amaranth determination, including thin layer chromatography, TCL [8]; high performance liquid chromatography mass spectrometry, HPLC-MS [9, 10]; electrochemical analysis [11–13]; liquid chromatography-tandem mass spectrometry, LC-MS [14, 15] and spectrophotometery [16]. Some advantages made electrochemical method interesting in this regard, including easy to use, no need for complicated equipment, low waste emissions, and possibility of miniaturization, rapidity and cost-effectiveness [17–19]. The electrode modification may be involved in the improvement of electrochemical sensor sensitivity for detection in the trace level. The chemical modification triggers electron transfer and thus induces electrocatalytic properties of the electrode surface and decreases the surface fouling [20–22].

Screen printed electrodes (SPEs) are used effectively in the construction of new electroanalytical methods due to their unique properties compared to other conventional electrodes, including the ability to connect to portable devices, high sensitivity, ability to act at ambient temperature, quick response, need for low power, linear output, possibility of miniaturization, commercial availability, cost-effectiveness and easy to use, reproducibility and high repeatability [23–25].

Metal–organic frameworks (MOF) are involved in the connection of metal nodes and organic linker, with regular structures bearing uniformly dispersed components and controllable pore size [26, 27]. Availability of metal active sites to rapidly electron/ion transfer is possible by MOFs due to the porous networks and large surface area. The fabrication of highly active metal electrocatalysts is possible with the controlled design and production of MOF-based materials. Synergetic impact of various metal sites on the surface of electrocatalysts makes hybrid bimetallic MOFs important materials to construct highly active electrocatalysts [28–30].

Therefore, the present study aimed to apply Ni and Mo as bimetallic ions for the synthesis of Ni–Mo-MOF to increase the framework stability and improve the catalytic properties through dispersion of active sites and coupling impact between the two metals, probably resulting in the introduction of a highly sensitive sensor for the amaranth detection.

Empirical protocols

Chemicals and devices

Electrochemical properties were evaluated by Eco Chemie Autolab PGSTAT30 Potentiostat/Galvanostat System, the Netherlands. The empirical conditions were monitored by general purpose electrochemical system (GPES) software. DropSens screen-printed electrodes (SPEs, DRP-110: Spain) included three unmodified graphite working electrode and graphite counter electrode and silver pseudo-reference electrode. The pH values were measured by a pH meter (Metrohm model 710).

Amaranth and all other reagents used were of analytical grade. They were purchased from Merck and Sigma-Aldrich companies with highest available purity. Orthophosphoric acid as well as the related salts, which are above the pH range of 2.0–9.0 are utilized to prepare the solutions of buffer. Water was deionized by a Nano Pure System (Barnstead).

Preparation of Ni–Mo-MOF

Co-precipitation method as performed for the fabrication of MOF at ambient temperature simultaneously by adding 100 mL of 0.01 M $K_2[Ni(CN)_4]$ and 100 mL of 0.1 M ammonium molybdate tetrahydrate to H_2O (200 mL) as dropwise, thereby forming precipitates immediately. The resulting precipitates were isolated, and then the impurity ions (such as K^+) were excluded by washing precipitates several times with deionized water, followed by drying in a vacuum oven at 60 °C.

Preparation of electrode

The bare SPE was coated by the Ni–Mo-MOF in accordance with a simplified process. Thus, the Ni–Mo-MOF (1 mg) was dispersed in aqueous solution (1 mL) under ultrasonication for 40 min. Then, the suspension (5 µL) was dropped onto the surfaces of carbon working electrode, finally followed by drying the solution at ambient temperature.

Preparation of real specimens

Orange juices and apple juices were purchased from local stores in Kerman, Iran, and used directly after filtration and without any pretreatment. We collected the tap water from our laboratory and analyzed it within 12 h. Before the analysis, the water has been filtered via a 0.22 µM cellulose acetate membrane. Then, each sample solution was poured individually into buffer solutions at pH value of 7.0 tested as real specimens.

Result and discussion

Electrochemical profile of amaranth on Ni–Mo-MOF

The optimum pH value must be determined to achieve acceptable outputs to check the pH-dependent electrochemical profile of amaranth. Thus, the experiments were

performed by modified electrode using different pH values (2.0–9.0). At last, the best outputs for amaranth electrooxidation were related to the pH of 7.0.

Figure 1 shows the CVs for the oxidation of amaranth on Ni–Mo-MOF/SPE (a) and bare SPE in the presence of 0.1 M PBS containing 100.0 µM of amaranth at the pH value of 7.0 and the scan rate of 50 mV s^{-1}. The oxidation of amaranth showed the anodic peak potential of 860 mV on the bare SPE, but 660 mV on the Ni–Mo-MOF/SPE. In fact, 200 mV decrease confirms highly effective electrocatalytic activity of Ni–Mo-MOF material regarding the amaranth oxidation.

Effect of scan rate on the results

The oxidation peak current is elevated by raising the scan rate, as can be seen in the results from the evaluation of potential scan rate impact on the amaranth oxidation currents (Fig. 2). Moreover, a linear relationship was found between Ip and the square root of potential scan rate ($\nu^{1/2}$), indicating that the analyst oxidation is in the control of diffusion.

Tafel plot was drawn using data from ascending domain of current/voltage curve, recorded at a scan rate of 10 mV s^{-1} for amaranth (Fig. 3). This section of voltammogram (Tafel region) has been influenced by the kinetics of electron transfer between amaranth and Ni–Mo-MOF/SPE. The Tafel slope was obtained to be 0.1567 V. This result is in line with the involvement of an electron at a rate indicating the electrode process phase, which presents the charge transfer coefficients of $\alpha = 62$ for the amaranth.

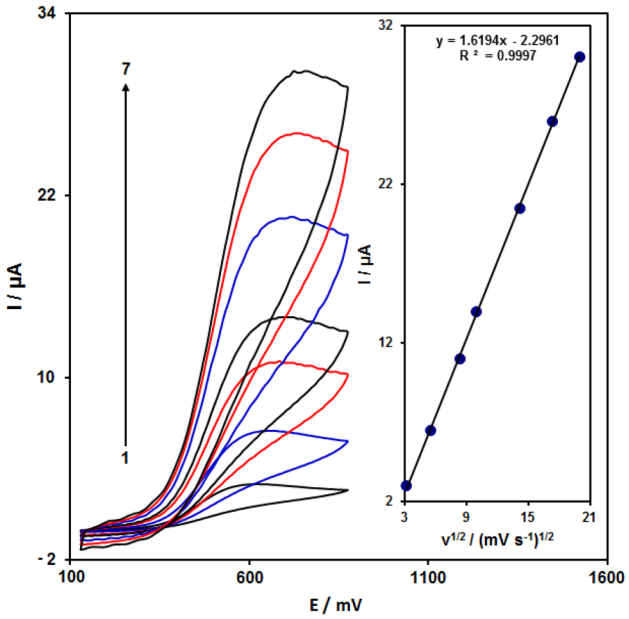

Fig. 2 CVs of Ni-Mo-MOF/SPE in exposure to amaranth (100.0 µM) in 0.1 M PBS at pH = 7.0 at different scan rates (numbers 1–7: 10, 30, 70, 100, 200, 300 and 400 mV s^{-1}), Insets: variation in anodic peak current versus square root of scan rate

Chronoamperometry

Ni–Mo-MOF /SPE at 710 mV were applied for chronoamperometric analysis of amaranth samples at different

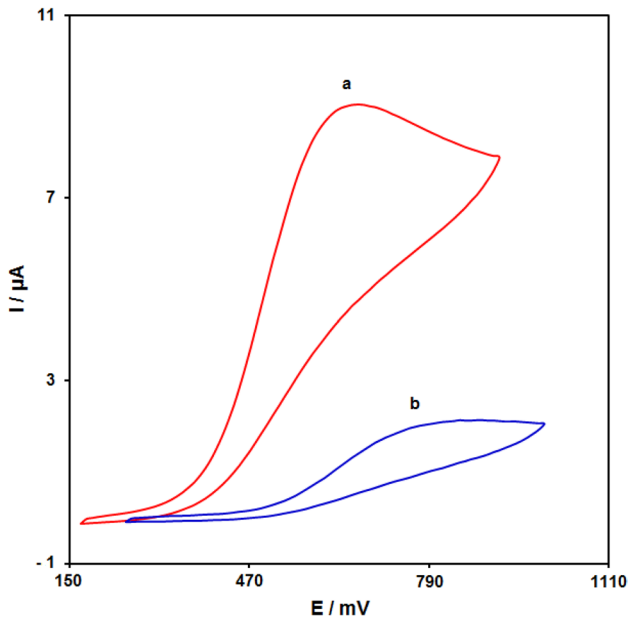

Fig. 1 CVs of Ni-Mo-MOF/SPE (a) and bare screen printed electrode (b) in exposure to amaranth (100.0 µM) at pH = 7.0, with the scan rate of 50 mV s^{-1}

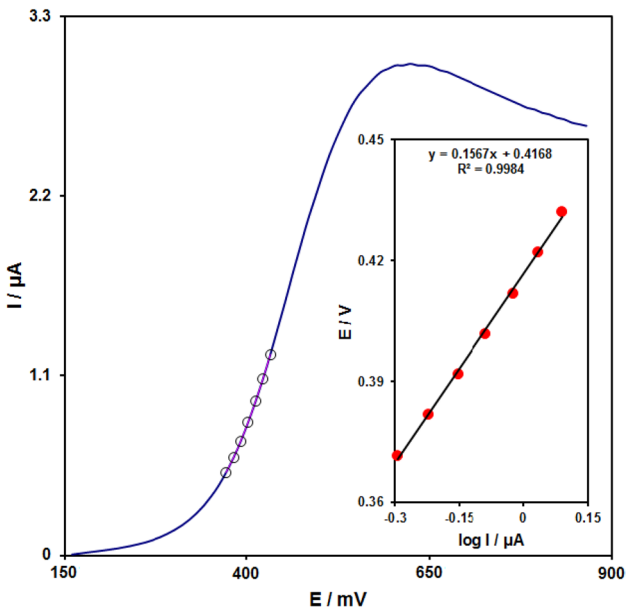

Fig. 3 LSV of electrode at 10 mV s^{-1} in exposure to amaranth (100.0 µM) in 0.1 M PBS at pH = 7.0; points: data applied in Tafel plot; inset: Tafel plot from linear sweep voltammetry

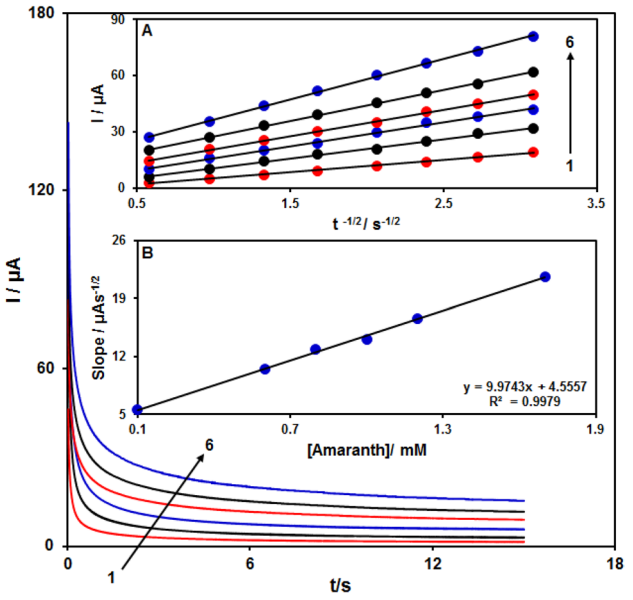

Fig. 4 Chronoamperograms gained at Ni-Mo-MOF/SPE in exposure to different amaranth concentrations (numbers 1–6: 0.1, 0.6, 0.8, 1.0, 1.2 and 1.7 mM) in 0.1 M PBS at pH = 7.0; Insets: (A) I versus $t^{-1/2}$ plots from chronoamperograms 1–6; (B) slope plot of straight lines versus amaranth concentrations

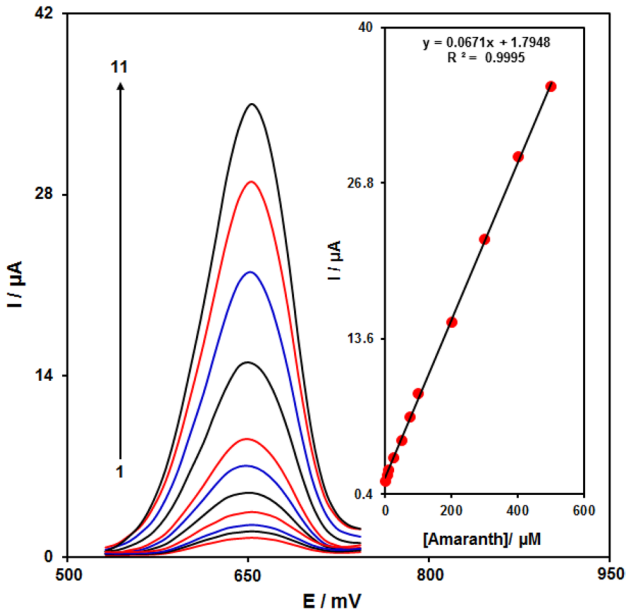

Fig. 5 Differential pulse voltammetry of Ni–Mo-MOF/SPE in exposure to different amaranth concentrations (numbers 1–11: 0.15, 5.0, 10.0, 25.0, 50.0, 75.0, 100.0, 200.0 300.0, 400.0 and 500.0 µM) in 0.1 M PBS at pH = 7.0; Inset: peak current plot as a concentration function of amaranth in range of 0.15–500.0 µM

concentrations in PBS (pH 7.0), as shown in Fig. 4. The chronoamperometric study of electroactive moieties in mass transfer limited conditions is based on Cottrell equation:

$$I = nFAD^{1/2}C_b\pi^{-1/2}t^{-1/2}$$

In this equation, D stands for diffusion coefficient ($cm^2\ s^{-1}$) and C_b for applied bulk concentration ($mol\ cm^{-3}$). Empirical data from I versus $t^{-1/2}$ plot were drawn in Fig. 4A, having the optimal fits for different amaranth concentrations. The slopes related to straight lines in Fig. 4A were drawn versus the amaranth concentration, as in Fig. 4B. Based on the Cottrell equation and the obtained slope, the mean D value was estimated at $1.03 \times 10^{-6}\ cm^2\ s^{-1}$. This value is comparable with the values reported in some previous works ($3.05 \times 10^{-6}\ cm^2\ s^{-1}$ [31] and $2.01 \times 10^{-6}\ cm^2\ s^{-1}$ [32]).

Calibration curve

The relationship between different amaranth concentrations and peak current was evaluated by the DPV method. The DPVs corresponding to Ni–Mo-MOF/SPE exposed to distinct amaranth concentration were recorded at different concentrations of 0.15 ± 0.001 to 500.0 ± 0.001 µM (Fig. 5). The amaranth determination on the Ni–Mo-MOF/SPE surface showed the limit of detection (LOD) of 0.05 ± 0.001 µM. Table 1 presents a comparison of voltammetric techniques for the detection of amaranth at the prepared electrode in this work and some other works.

Interference study

The impact of numerous interference substances on the determination of amaranth was investigated. The tolerance limit was taken as the maximum of the foreign materials concentration that resulted about ± 5% relative error in the determination. The results indicated that glucose, sucrose, L-threonine, alanine, glycine, guanine, tryptophan, Sudan I, Na^+, Cl^-, K^+, Mg^{2+}, NO_3^- did not affect the response. Therefore, the proposed sensor has an excellent selectivity for detection of amaranth.

Experiments on real samples

At last, the applicability of a novel electrochemical sensor of Ni–Mo-MOF/SPE was examined by the detection of amaranth in different real specimens, i.e. fruit juices and water resources. As shown in Table 2, the attained recovery data confirmed the potential of sensitive Ni–Mo-MOF/SPE sensor in the determination of amaranth present in the real specimens.

Table 1 A comparison of the efficiency of Ni–Mo-MOF/SPE and various modified electrodes reported for the detection of amaranth

Electrochemical sensor	Method	Linear dynamic range	Limit of detection	Ref
Multi-wall carbon nanotube thin film/gold electrode	DPV	1.0×10^{-5}–1.0×10^{-6} M	6.8×10^{-8} M	[7]
Poly(sodium p-styrenesulfonate)-graphene-Pd/glassy carbon electrode	DPV	1×10^{-7}–9×10^{-6} M	7 nM	[12]
Fe_3O_4@reduced graphene oxide/glassy carbon electrode	DPV	0.05–50 µM	50 nM	[33]
Multi-wall carbon nanotube thin film/glassy carbon electrode	DPV	40 nM–0.8 µM	35 nM	[34]
Single-wall carbon nanotube-titanium nitride nanocomposite/glassy carbon electrode	DPV	0.1–100 µM	40 nM	[35]
Ni–Mo-MOF/SPE	DPV	0.15–500.0 µM	0.05 µM	This work

Table 2 Amaranth detection in real specimens via Ni–Mo-MOF/SPE at different concentrations (µM) (n = 5)

R.S.D. (%)	Recovery (%)	Found	Spiked	Sample
–	–	–	0	Orange juice
3.2 ± 0.1	98.0 ± 0.5	4.9	5.0	
2.4 ± 0.1	104.0 ± 0.5	7.8	7.5	
1.7 ± 0.1	101.0 ± 0.5	10.1	10.0	
2.1 ± 0.1	99.2 ± 0.5	12.4	12.5	
–	–	–	0	Apple juice
2.4 ± 0.1	102.5 ± 0.5	4.1	4.0	
3.0 ± 0.1	98.3 ± 0.5	5.9	6.0	
2.0 ± 0.1	103.7 ± 0.5	8.3	8.0	
2.6 ± 0.1	99.0 ± 0.5	9.9	10.0	
–	–	–	0	Tap water
3.5 ± 0.1	96.0 ± 0.5	4.8	5.0	
1.9 ± 0.1	101.0 ± 0.5	10.1	10.0	
2.2 ± 0.1	99.3 ± 0.5	14.9	15.0	
2.8 ± 0.1	102.5 ± 0.5	20.5	20.0	

Conclusion

In this work, we have successfully synthesized the Ni–Mo-MOF. A SPE was modified with Ni-Mo-MOF to fabricate the amaranth sensor. As determined by CV, Ni–Mo-MOF/SPE exhibited excellent electrochemical oxidation towards the detection of amaranth. Acquired DPV results at Ni–Mo-MOF showed a respectable linear range of 0.15 ± 0.001–500.0 ± 0.001 µM, lower LOD of 0.05 ± 0.001 µM, the higher sensitivity of 0.0671 µA μM^{-1}. Notably, the proposed method presented good selectivity for the determination of amaranth. According to the proposed protocol, appropriate recoveries were found to detect the amaranth in real samples.

Acknowledgements This research was supported by Kerman University of Medical Sciences, Kerman, Iran and the National Research Foundation of Korea (NRF) funded by the Ministry of Science and ICT (2020M2D8A206983011). Furthermore, financial support from the Basic Science Research Program (2017R1A2B3009135) through the National Research Foundation of Korea is appreciated.

Declarations

Conflict of interest The authors declare that they have no conflict of interest.

References

1. W.R. Barros, P.C. Franco, J.R. Steter, R.S. Rocha, M.R. Lanza, Electro-Fenton degradation of the food dye amaranth using a gas diffusion electrode modified with cobalt(II) phthalocyanine. J. Electroanal. Chem. **722**, 46–53 (2014)
2. M. Wang, M. Cui, M. Zhao, H. Cao, Sensitive determination of Amaranth in foods using graphene nanomeshes. J. Electroanal. Chem. **809**, 117–124 (2018)
3. S. Tvorynska, B. Josypčuk, J. Barek, L. Dubenska, Electrochemical behavior and sensitive methods of the voltammetric determination of food azo dyes amaranth and allura red AC on amalgam electrodes. Food Anal. Methods **12**, 409–421 (2019)
4. S. Jing, H. Zheng, L. Zhao, L. Qu, L. Yu, Electrochemical sensor based on poly (sodium 4-styrenesulfonate) functionalized graphene and Co_3O_4 nanoparticle clusters for detection of amaranth in soft drinks. Food Anal. Methods **10**, 3149–3157 (2017)
5. L. Li, H. Zheng, L. Guo, L. Qu, L. Yu, A sensitive and selective molecularly imprinted electrochemical sensor based on Pd–Cu bimetallic alloy functionalized graphene for detection of amaranth in soft drink. Talanta **197**, 68–76 (2019)
6. Q. He, J. Liu, X. Liu, G. Li, P. Deng, J. Liang, Manganese dioxide Nanorods/electrochemically reduced graphene oxide nanocomposites modified electrodes for cost-effective and ultrasensitive detection of Amaranth. Colloid. Surf B Biointerfaces **172**, 565–572 (2018)
7. S. Chandran, L.A. Lonappan, D. Thomas, T. Jos, K.G. Kumar, Development of an electrochemical sensor for the determination of amaranth: a synthetic dye in soft drinks. Food Anal. Method. **7**, 741–774 (2014)
8. W.W. Tonica, M.F. Hardianti, S.A. Prasetya, O. Rachmaniah, Determination of Rhodamine-B and Amaranth in snacks at primary school Sukolilo district of Surabaya-Indonesia by thin layer chromatography, in AIP Conference Proceedings, vol. 2049 (AIP Publishing LLC, 2018), p. 020043
9. M. Ma, X. Luo, B. Chen, S. Su, S. Yao, Simultaneous determination of water-soluble and fat-soluble synthetic colorants in foodstuff by high-performance liquid chromatography–diode array detection–electrospray mass spectrometry. J. Chromatogr. A **1103**, 170–176 (2006)
10. X.Q. Li, Q.H. Zhang, K. Ma, H.M. Li, Z. Guo, Identification and determination of 34 water-soluble synthetic dyes in foodstuff by high performance liquid chromatography–diode array

detection–ion trap time-of-flight tandem mass spectrometry. Food Chem. **182**, 316–326 (2015)
11. F. Pogacean, M.C. Rosu, M. Coros, L. Magerusan, M. Moldovan, C. Sarosi, S. Pruneanu, Graphene/TiO_2-Ag based composites used as sensitive electrode materials for amaranth electrochemical detection and degradation. J. Electrochem. Soc. **165**, B3054 (2018)
12. Y. Gao, L. Wang, Y. Zhang, L. Zou, G. Li, B. Ye, Electrochemical behavior of amaranth and its sensitive determination based on Pd-doped polyelectrolyte functionalized graphene modified electrode. Talanta **168**, 146–151 (2017)
13. M. Wang, Y. Gao, Q. Sun, J. Zhao, Ultrasensitive and simultaneous determination of the isomers of Amaranth and Ponceau 4R in foods based on new carbon nanotube/polypyrrole composites. Food Chem. **172**, 873–879 (2015)
14. K.H. Park, J.H. Choi, A.M. Abd El-Aty, S.K. Cho, J.H. Park, B.M. Kim, J.H. Shim, Determination of spinetoram and its metabolites in amaranth and parsley using QuEChERS-based extraction and liquid chromatography–tandem mass spectrometry. Food Chem. **134**, 2552–2559 (2012)
15. F. Feng, Y. Zhao, W. Yong, L. Sun, G. Jiang, X. Chu, Highly sensitive and accurate screening of 40 dyes in soft drinks by liquid chromatography–electrospray tandem mass spectrometry. J. Chromatogr. B **879**, 1813–1818 (2011)
16. A.A. El-Zomrawy, Selective and sensitive spectrophotometric method to determine trace amounts of copper metal ions using Amaranth food dye. Spectrochim. Acta Part A Mol. Biomol. Spectrosc. **203**, 450–454 (2018)
17. Q.Q. Hu, H. Gao, Y.M. Wang, W. Ma, D.M. Sun, Simultaneous determination of Carmine and Amaranth based on a poly (L-Arginine)–graphene modified electrode. J. Anal. Chem. **73**, 817–823 (2018)
18. Y. Gao, H. Li, J. Tong, L. Wang, A new voltammetric sensor based on poly (L-cysteine)/GR composite film modified electrode for the sensitive determination of amaranth in wastewater. Environ. Technol. **42**, 2385–2390 (2021)
19. I. Elaissaoui, H. Akrout, S. Grassini, D. Fulginiti, L. Bousselmi, Effect of coating method on the structure and properties of a novel PbO_2 anode for electrochemical oxidation of Amaranth dye. Chemosphere **217**, 26–34 (2019)
20. H. Karimi-Maleh, M. Alizadeh, Y. Orooji, F. Karimi, M. Baghayeri, J. Rouhi, S. Tajik, H. Beitollahi, S. Agarwal, V.K. Gupta, S. Rajendran, S. Rostamnia, L. Fu, F. Saberi-Movahed, S. Malekmohammadi, Ind. Eng. Chem. Res. **60**, 816–823 (2021)
21. M. Sajid, N. Baig, K. Alhooshani, Chemically modified electrodes for electrochemical detection of dopamine: challenges and opportunities. TrAC Trend. Anal. Chem. **118**, 368–385 (2019)
22. H. Karimi-Maleh, M.L. Yola, N. Atar, Y. Orooji, F. Karimi, P.S. Kumar, J. Rouhi, M. Baghayeri, J. Colloid Interface Sci. **592**, 174–185 (2021)
23. M. Singh, N. Jaiswal, I. Tiwari, C.W. Foster, C.E. Banks, A reduced graphene oxide-cyclodextrin-platinum nanocomposite modified screen printed electrode for the detection of cysteine. J. Electroanal. Chem. **829**, 230–240 (2018)
24. I.M. Apetrei, C. Apetrei, A modified nanostructured graphene-gold nanoparticle carbon screen-printed electrode for the sensitive voltammetric detection of rutin. Measurement **114**, 37–43 (2018)
25. Y. Zhang, X. Jiang, J. Zhang, H. Zhang, Y. Li, Simultaneous voltammetric determination of acetaminophen and isoniazid using MXene modified screen-printed electrode. Biosens. Bioelectron. **130**, 315–321 (2019)
26. W.J. Dang, Y.Q. Shen, M. Lin, H. Jiao, L. Xu, Z.L. Wang, Noble-metal-free electrocatalyst based on a mixed CoNi metal-organic framework for oxygen evolution reaction. J. Alloy. Compd. **792**, 69–76 (2019)
27. Q. Li, H. Guo, R. Xue, M. Wang, M. Xu, W. Yang, W. Yang, Self-assembled Mo doped Ni-MOF nanosheets based electrode material for high performance battery-supercapacitor hybrid device. Int. J. Hydrogen Energy **45**, 20820–20831 (2020)
28. K. Zhou, D. Shen, X. Li, Y. Chen, L. Hou, Y. Zhang, J. Sha, Molybdenum oxide-based metal-organic framework/polypyrrole nanocomposites for enhancing electrochemical detection of dopamine. Talanta **209**, 120507 (2020)
29. J. Xu, Q. Ji, X. Yan, C. Wang, L. Wang, Ni (acac) 2/Mo-MOF-derived difunctional MoNi@ MoO_2 cocatalyst to enhance the photocatalytic H_2 evolution activity of g-C_3N_4. Appl. Catal. B Environ. **268**, 118739 (2020)
30. Y. Li, K. Pascal, X.J. Jin, Ni–Mo modified metal–organic frameworks for high-performance supercapacitance and enzymeless H_2O_2 detection. Cryst. Eng. Comm. **22**, 5145–5161 (2020)
31. M. Sheikhshoaie, H. Karimi-Maleh, I. Sheikhshoaie, M. Ranjbar, Voltammetric amplified sensor employing RuO_2 nano-road and room temperature ionic liquid for amaranth analysis in food samples. J. Mol. Liq. **229**, 489–494 (2017)
32. M. Bijad, H. Karimi-Maleh, M. Farsi, S.A. Shahidi, Simultaneous determination of amaranth and nitrite in foodstuffs via electrochemical sensor based on carbon paste electrode modified with CuO/SWCNTs and room temperature ionic liquid. Food Anal. Methods **10**, 3773–3780 (2017)
33. Q. Han, X. Wang, Z. Yang, W. Zhu, X. Zhou, H. Jiang, Fe_3O_4@rGO doped molecularly imprinted polymer membrane based on magnetic field directed self-assembly for the determination of amaranth. Talanta **123**, 101–108 (2014)
34. P. Wang, X. Hu, Q. Cheng, X. Zhao, X. Fu, K. Wu, Electrochemical detection of amaranth in food based on the enhancement effect of carbon nanotube film. J. Agric. Food Chem. **58**, 12112–12116 (2010)
35. J.L. He, W. Kou, C. Li, J.J. Cai, F.Y. Kong, W. Wang, Electrochemical sensor based on single-walled carbon nanotube-TiN nanocomposites for detecting Amaranth. Int. J. Electrochem. Sci. **10**, 10074–10082 (2015)